

# M33 – Distance and Motion

Andreas Brunthaler

Joint Institute for VLBI in Europe  
Postbus 2, 7990 AA Dwingeloo, the Netherlands  
brunthaler@jive.nl

## Abstract

*Measuring the proper motions and geometric distances of galaxies within the Local Group is very important for our understanding of the history, present state and future of the Local Group. Currently, proper motion measurements using optical methods are limited only to the closest companions of the Milky Way. However, Very Long Baseline Interferometry (VLBI) provides the best angular resolution in astronomy and phase-referencing techniques yield astrometric accuracies of  $\approx 10$  microarcseconds. This makes a measurement of proper motions and angular rotation rates of galaxies out to a distance of  $\sim 1$  Mpc feasible.*

*This article presents results of VLBI observations of two regions of  $H_2O$  maser activity in the Local Group galaxy M33. The two masing regions are on opposite sides of the galaxy. This allows a comparison of the angular rotation rate (as measured by the VLBI observations) with the known inclination and rotation speed of the HI gas disk. This gives a geometric distance of  $730 \pm 100 \pm 135$  kpc. The first error indicates the statistical error from the proper motion measurements while the second error is the systematic error from the rotation model. This distance is consistent, within the errors, with the most recent Cepheid distance to M33. Since all position measurements were made relative to an extragalactic background source, the proper motion of M33 has also been measured. This provides a three dimensional velocity vector of M33, showing that this galaxy is moving with a velocity of  $190 \pm 59$  km s $^{-1}$  relative to the Milky Way. These measurements promise a new handle on dynamical models for the Local Group and the mass and dark matter halo of Andromeda and the Milky Way.*

## 1 Introduction

The nature of spiral nebulae like M33 was the topic of a famous debate in the 1920's. While some astronomers favored a close distance and Galactic origin, others were convinced of the extragalactic nature. In 1923, van Maanen claimed to have measured a large proper motion and angular rotation of M33 from photographic plates separated by  $\approx 12$  years. These measurements yielded rotational motions of  $\approx 10$ -30 mas yr $^{-1}$ , clearly indicating a close distance to M33. However, Hubble (1926) discovered Cepheids in M33, showing a large distance to M33 and confirming that M33 is indeed an extragalactic object. The expected proper motions from the rotation of M33 are only  $\approx 30$   $\mu$ as yr $^{-1}$ , and 3 orders of magnitude smaller than the motions claimed by van

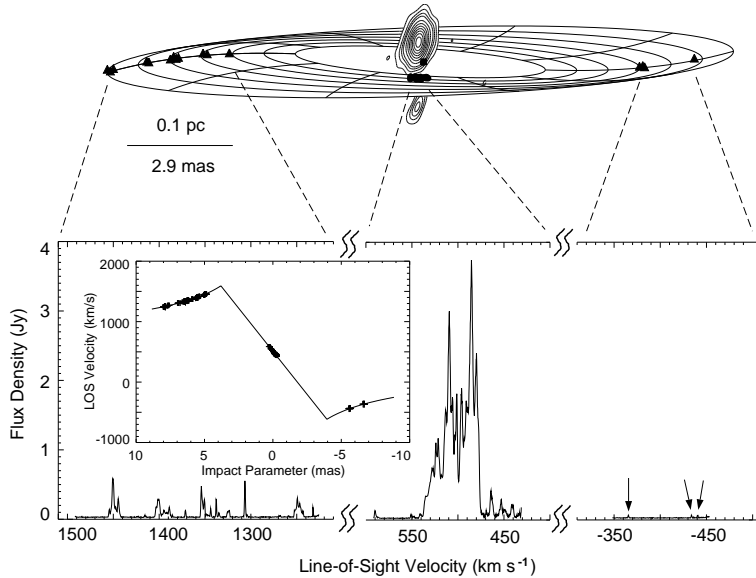


Figure 1: The warped disk model for NGC 4258. The inset shows line-of-sight (LOS) velocity versus impact parameter for the best-fitting Keplerian disk, with the maser data superposed (taken from Herrnstein et al. (1999)).

Maanen. The source of error in van Maanens observations was never identified. After more than 80 years, the idea behind the experiment to measure the rotation and proper motions of galaxies remains interesting for our understanding of the dynamics and geometry of the Local Group. Hence, they are an important science goal of future astrometric missions, e.g. the Space Interferometry Mission (SIM, see Shaya et al. 2003).

## 1.1 Geometric Distances

Currently, the calibration of most standard candles used for extragalactic distances, are tied in one way or another to the distance of the Large Magellanic Cloud (LMC) (e.g., Freedman 2000; Mould et al. 2000). However, recently Tammann, Sandage, & Reindl (2003) and Sandage, Tammann, & Reindl (2004) find differences in the slopes of the Period – Luminosity (P–L) relations in Cepheids in the Galaxy, LMC and SMC. This “weakens the hope of using Cepheids to attain good accuracies in measuring galaxy distances” until the reasons for the differences in the P–L relations are understood. This has been also confirmed by Ngeow & Kanbur (2004).

Hence, geometric distances to nearby galaxies in which well understood standard candles can be studied, are needed to limit systematic errors in the extragalactic distance scale. However, geometric distances to other galaxies

are very difficult to obtain. The best case is the Seyfert galaxy NGC 4258. Here, water vapor maser emission in a Keplerian circumnuclear disk that orbits a super-massive black hole in the center of the galaxy (see Fig. 1) was used to measure a geometric distance. This distance of  $7.2 \pm 0.5$  Mpc (Herrnstein et al. 1999) is slightly shorter than the distance estimate using Cepheids by Newman et al. (2001) who derive a value of  $7.8 \pm 0.3$  Mpc.

To confirm and calibrate the current extragalactic distance scale it is essential to obtain geometric distances to other nearby galaxies. This involves detection of coherent motions at extragalactic distances.

## 1.2 Proper Motions

Another important astrophysical question is the nature and existence of dark matter in the universe. The existence of dark matter was first suggested in the 1930s by Fritz Zwicky from the observed peculiar motions of galaxies in clusters. It was firmly established by observations of the flat rotation curves of galaxies (e.g. Fich & Tremaine 1991). The closest place to look for dark matter halos is the Milky Way and Andromeda in the Local Group. Various attempts have been made to weigh the galaxies in the Local Group and determine size and mass of the Milky Way and its not very prominent dark matter halo (Kulesa & Lynden-Bell 1992; Kochanek 1996). Other attempts use Local Group dynamics in combination with MACHO data to constrain the universal baryonic fraction (Steigman & Tkachev 1999).

The problem when trying to derive the gravitational potential of the Local Group is that usually only radial velocities are known and hence statistical approaches have to be used. Kulesa & Lynden-Bell (1992) introduced a maximum likelihood method which requires only the line-of-sight velocities, but it is also based on some assumptions (eccentricities, equipartition).

Clearly, the most reliable way of deriving masses is using orbits, which requires the knowledge of three-dimensional velocity vectors obtained from measurements of proper motions. The usefulness of proper motions was impressively demonstrated for the Galactic Center where the presence of a dark mass concentration, presumably a super-massive black hole, has been unambiguously demonstrated by stellar proper motion measurements (Eckart & Genzel 1996; Schödel et al. 2002; and Ghez et al. 2003).

However, measuring proper motions of members of the Local Group to determine its mass is difficult. For the LMC Jones, Klemola, & Lin (1994) claim a proper motion of  $1.2 \pm 0.28$  mas yr<sup>-1</sup> obtained from comparing photographic plates over a time-span of 14 years. Schweitzer et al. (1995) claim  $0.56 \pm 0.25$  mas yr<sup>-1</sup> for the Sculptor dwarf spheroidal galaxy from plates spanning 50 years in time (Fig 2). Kochanek (1996) shows that inclusion of these marginal proper motions can already significantly improve the estimate for the mass of the Milky Way, since it reduces the strong ambiguity caused by Leo I, which can be treated as either bound or unbound to the Milky Way. The same work also concludes that if the claimed optical proper motions are true, the models also predict a relatively large tangential velocity of the other

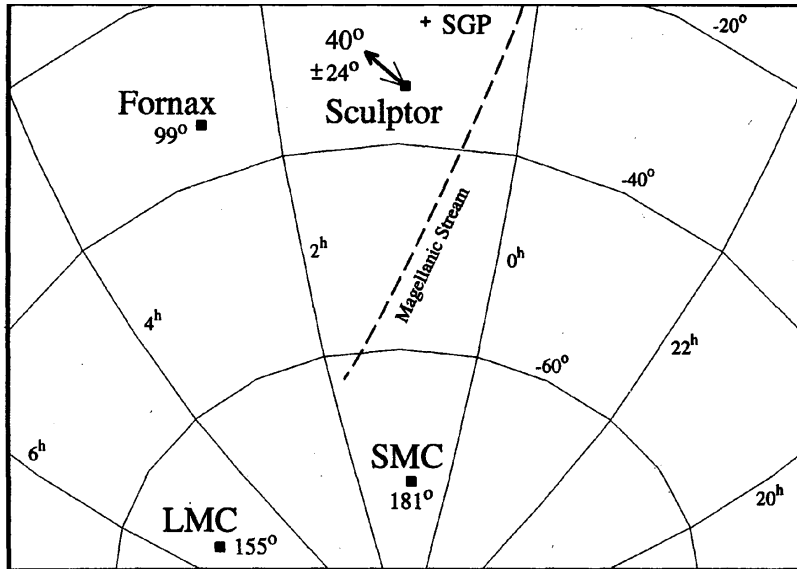


Figure 2: The proper motion of the Sculptor Dwarf Spheroidal Galaxy. Taken from Schweitzer et al. (1995).

satellites of the Galaxy.

The dynamics of nearby galaxies are also important to determine the solar motion with respect to the Local Group to help define a standard inertial reference frame (Courteau & van den Bergh 1999). And again, as Courteau and van den Bergh point out, “interpretation errors for the solar motion may linger until we obtain a better understanding of the true orbital motion of Local Group members”.

Despite the promising start, the disadvantage of the available optical work is obvious: a further improvement and confirmation of these measurements requires an additional large time span of many decades and will still be limited to only the closest companions of the Milky Way.

### 1.3 Proper Motions with VLBI

On the other hand, the expected proper motions for galaxies within the Local Group, ranging from  $0.02 - 1 \text{ mas yr}^{-1}$ , can be seen with Very Long Baseline Interferometry (VLBI) using the phase-referencing technique. A good reference point is the motion of Sgr A\* across the sky reflecting the Sun’s rotation around the Galactic Center. This motion is well detected between epochs separated by only one month with the VLBA (Reid et al. 1999). New observations increased the time span to 8 years. The position of Sgr A\* relative to the background quasar J1745-283 is shown in Figure 3 (taken from Reid &

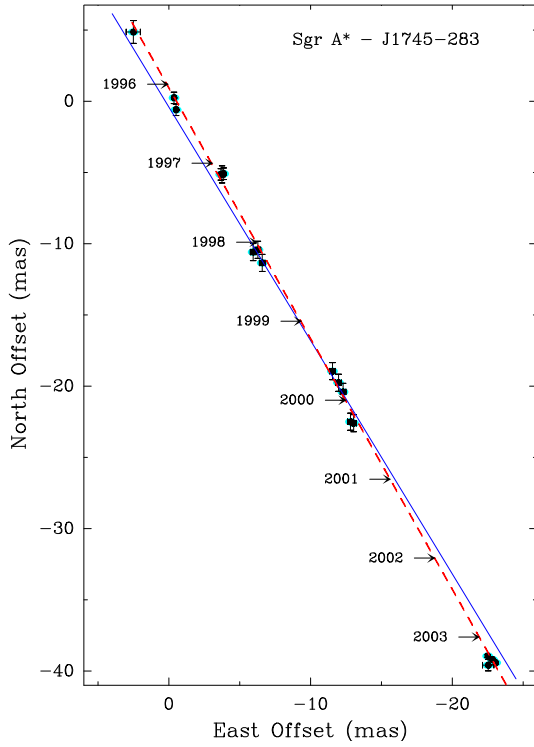


Figure 3: Apparent motion of Sgr A\* relative to a background quasar. The blue line indicates the orientation of the Galactic plane and the dashed line is the variance-weighted best-fit proper motion.

Brunthaler 2004).

The motion of Sgr A\* is  $6.379 \pm 0.026 \text{ mas yr}^{-1}$  and almost entirely in the plane of the galaxy. This gives, converted to Galactic coordinates a proper motion of  $-6.379 \pm 0.026 \text{ mas yr}^{-1}$  in Galactic longitude and  $-0.202 \pm 0.019 \text{ mas yr}^{-1}$  in Galactic latitude. If one assumes a distance to the Galactic Center ( $R_0$ ) of  $8 \pm 0.5 \text{ kpc}$  (e.g. Reid 1993, Eisenhauer et al. 2003), these motions translate to a velocity of  $-241 \pm 15 \text{ km s}^{-1}$  along the Galactic plane and  $-7.6 \pm 0.6 \text{ km s}^{-1}$  out of the plane of the Galaxy. This motion can be entirely explained by a combination of a circular rotation of the Local Standard of Rest (LSR)  $\Theta_0$  and the deviation of the motion of the Sun from the motion of the LSR. Removing the Solar motion relative to the LSR as measured by Hipparcos data by Dehnen & Binney (1998) ( $5.25 \pm 0.62 \text{ km s}^{-1}$  in longitude and  $-7.17 \pm \text{ km s}^{-1}$  in latitude) yields an estimate of  $\Theta_0 = 236 \pm 15 \text{ km s}^{-1}$ . Here the error is dominated by the uncertainty in the distance  $R_0$  to the Galactic Center. The motion of Sgr A\* out of the plane of the Galaxy is only  $-0.4 \pm 0.8 \text{ km s}^{-1}$ . This lower limit can be used to put tight constraints for

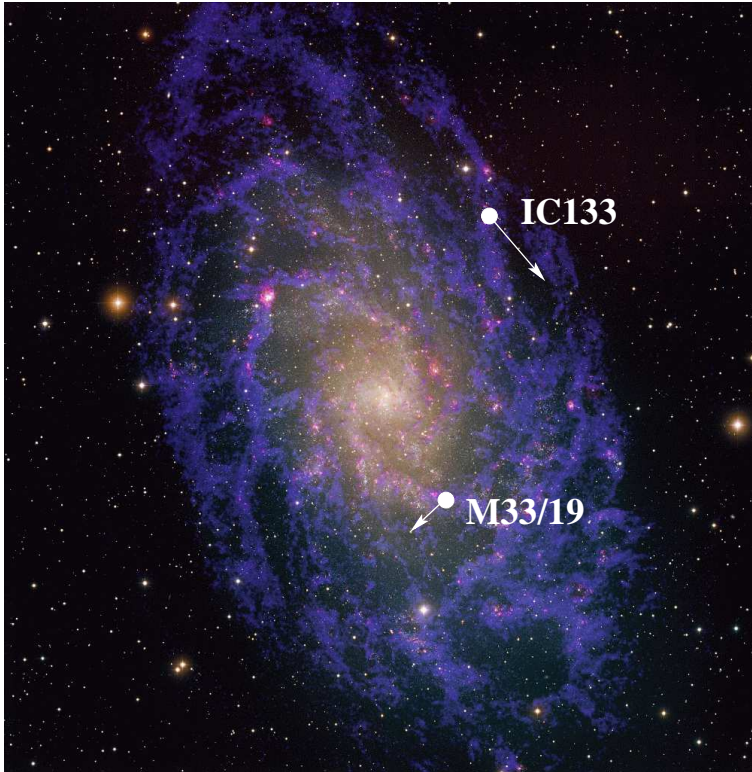


Figure 4: Position of two regions of maser activity in M33. Also shown are predicted motions due to rotation of the HI disk. The image of M33 was provided by Travis Rector (NRAO/AUI/NSF and NOAO/AURA/NSF), David Thilker (NRAO/AUI/NSF) and Robert Braun (ASTRON).

the mass of Sgr A\* (for details see Reid & Brunthaler 2004).

With the accuracy obtainable with VLBI one can in principle measure very accurate proper motions for most Local Group members within less than a decade. The main problem so far is finding appropriate radio sources. Useful sources would be either compact radio cores or strong maser lines associated with star forming regions. Fortunately, in a few galaxies bright masers are already known. Hence the task that lies ahead of us, if we want to significantly improve the Local Group proper motion data and mass estimate, is to make phase-referencing observations with respect to background quasars of known Local Group galaxies with strong H<sub>2</sub>O masers.

The most suitable candidates for such a VLBI phase-referencing experiment are the strong H<sub>2</sub>O masers in IC 10 ( $\sim 10$  Jy peak flux in  $0.5 \text{ km s}^{-1}$  line, the brightest known extragalactic maser; Becker et al. 1993) and IC 133 in M33 ( $\sim 2$  Jy, the first extragalactic maser discovered). Both masers have

Table 1: Details of the observations: Observing date, observation length  $t_{obs}$ , beam size  $\theta$  and position angle  $PA$  of the beam.

| Epoch | Date       | $t_{obs}$ | $\theta$ [mas]     | $PA$ [°] |
|-------|------------|-----------|--------------------|----------|
| I     | 2001/03/27 | 10 h      | $0.88 \times 0.41$ | 164      |
| I     | 2001/04/05 | 10 h      | $0.86 \times 0.39$ | 169      |
| II    | 2002/01/28 | 10 h      | $0.62 \times 0.33$ | 176      |
| II    | 2002/02/03 | 10 h      | $0.71 \times 0.33$ | 175      |
| III   | 2002/10/30 | 10 h      | $0.87 \times 0.38$ | 171      |
| III   | 2002/11/12 | 10 h      | $0.84 \times 0.36$ | 165      |
| IV    | 2003/12/14 | 12 h      | $0.85 \times 0.36$ | 159      |
| IV    | 2004/01/08 | 12 h      | $1.15 \times 0.47$ | 164      |

been observed successfully with VLBI (e.g. Argon et al. 1994, Greenhill et al. 1990, Greenhill et al. 1993, Brunthaler et al. 2002).

The two galaxies belong to the brightest members of the Local Group and are thought to be associated with M31. In both cases a relatively bright phase-referencing source is known to exist within a degree. In addition their galactic rotation is well known from HI observations. Consequently, M33 and IC 10 seem to be the best known targets for attempting to measure Local Group proper motions with the VLBA.

The next sections are based on Brunthaler et al. (2005) and present the first results of a program to measure the geometric distance and proper motion of M33. The results on IC 10 will be discussed in a subsequent paper.

## 2 VLBI observations of M33

### 2.1 Observations and Data Reduction

We observed two regions of H<sub>2</sub>O maser activity in M33, M33/19 (following the notation of Israel & van der Kruit 1974) and IC 133, eight times with the NRAO Very Long Baseline Array (VLBA) between March 2001 and January 2004. M33/19 is located in the south-eastern part of M33, while IC 133 is located in the north-east of M33 (see Fig. 4). Details of the observations are shown in Table 1. The observations are grouped into four epochs, each comprising two closely spaced observations to enable assessment of overall accuracy and systematic errors. The separations of the two observations within each epoch were large enough that the weather conditions are uncorrelated, but small enough that proper motions are negligible during this time.

We observed four 8 MHz bands, in dual circular polarization. The 128 spectral channels in each band yield a channel spacing of 62.5 kHz, equivalent to  $0.84 \text{ km s}^{-1}$ , and covered a velocity range of  $107 \text{ km s}^{-1}$ . The observations involved rapid switching between the phase-calibrator J0137+312,

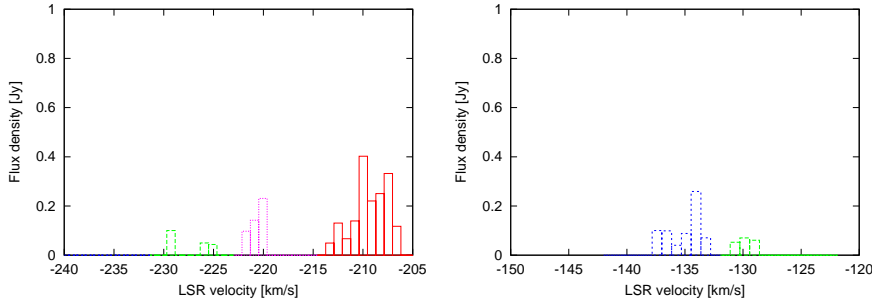


Figure 5: VLBI-spectrum of IC 133 (left) and M33/19 (right) on 2002 February 03.

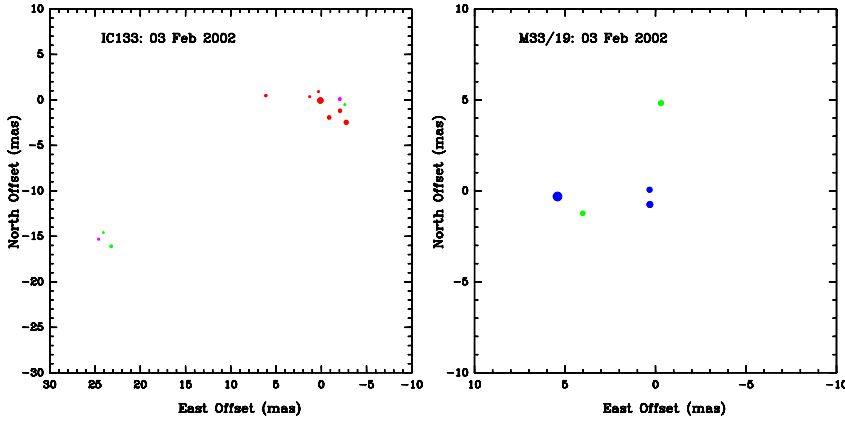


Figure 6: Composite map of the  $\text{H}_2\text{O}$  masers in IC 133 (left) and M33/19 (right). The area of the circles is proportional to the flux density of the components.

which is a compact background source with continuum emission, and the target sources IC 133 and M33/19 (J0137+312 – IC 133 – J0137+312 – M33/19 – J0137+312). With source changes every 30 seconds, an integration time of 22 seconds was achieved. The background source was assumed to be stationary on the sky. Being separated by only  $1^\circ$  on the sky from the masers, one can obtain a precise angular separation measurement for all sources. The data were edited and calibrated using standard techniques in the Astronomical Image Processing System (AIPS) as well as zenith delay corrections (see Brunthaler, Reid, & Falcke 2005 for discussion) to improve the accuracy of the phase-referencing. The masers in IC 133 and M33/19 were imaged with standard techniques in AIPS.

In IC 133, 29 distinct emission features were detected. The VLBI spectra and spatial distribution of the maser components in IC 133 in the observation



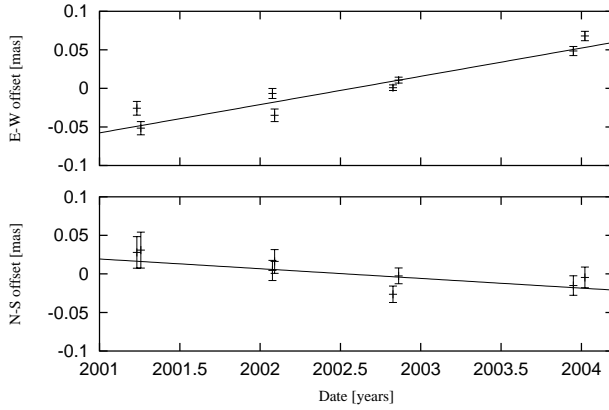


Figure 7: Average position of the masers M33/19 in right ascension (upper) and declination (lower) relative to a background source.

on 2004 February 03 are shown in Figures 5 and 6. Most maser components cluster in two regions, IC 133M (main) and IC 133SE (southeast), following the notation of Greenhill et al. (1990). These two regions are separated by  $\approx 30$  mas, which translates at an assumed distance of 790 kpc to  $3.5 \times 10^{17}$  cm. The emission in both regions is spread over  $\approx 4$  mas, corresponding to  $\approx 3200$  AU. This is similar to water maser emission in Galactic star-forming regions like W3(OH), W49 or Sgr B2 (e.g. Reid et al. 1995, Walker et al. 1977 and Kobayashi et al. 1989 respectively). The spectrum and the spatial distribution is very similar to earlier VLBI observations by Argon et al. (2004), Greenhill et al. (1990), and Greenhill et al. (1993). All components were unresolved.

In M33/19, 8 maser features (see Figures 5 and 6) could be detected. The two features near the phase center were separated by less than a beam size and blend together. These two features were fit by two elliptical Gaussian components simultaneously. All other features were fit by a single elliptical Gaussian component.

## 2.2 Proper Motions of M33/19 and IC 133

The maser emission in M33/19 and IC 133 is variable on timescales less than one year. Between the epochs, new maser features appeared while others disappeared. However, the motions of 4 components in M33/19 and 6 components in IC 133 could be followed over all four epochs. The component identification was based on the positions and radial velocities of the maser emission. Each component was usually detected in several frequency channels. A rectilinear motion was fit to each maser feature in each velocity channel separately. Fits with reduced  $\chi^2$  larger than 3 were discarded as they are likely affected by blending. Then, the variance weighted average of all motions was calculated. This yields an average motion of the maser components in M33/19 of 35.5

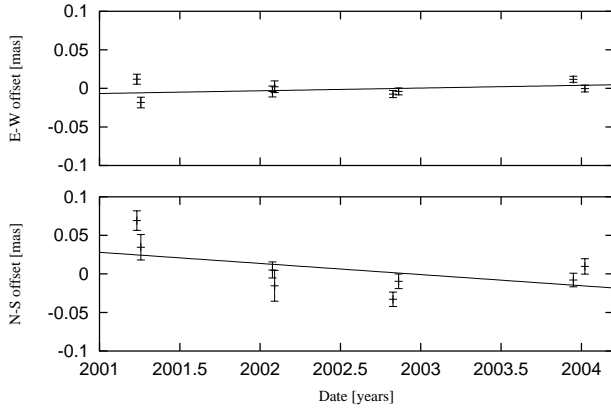


Figure 8: Average position of the masers in IC 133 in right ascension (upper) and declination (lower) relative to a background source.

$\pm 2.7 \mu\text{as yr}^{-1}$  in right ascension and  $-12.5 \pm 6.3 \mu\text{as yr}^{-1}$  in declination relative to the background source J0137+312. For IC 133 one gets an average motion of  $4.7 \pm 3.2 \mu\text{as yr}^{-1}$  in right ascension and  $-14.1 \pm 6.4 \mu\text{as yr}^{-1}$  in declination. All motions are on the plane of the sky. The larger uncertainty in declination is caused by the elliptical beam shape of the VLBA (see also Table 1). The accuracy and number of measured motions is not adequate to model the internal dynamics of the IC133 and M33/19 regions (e.g., outflow), as was done by Greenhill et al. (1993) and Argon et al. (2004). Though for now the internal dynamics are small enough to be in the noise, future observations that are more sensitive will have to incorporate dynamical models for each region.

One can also calculate the average position of all maser components for each observation. Here, the individual fits for each maser feature were used to remove a constant position difference for each maser feature. We used the position difference at epoch 2002.627, which is in the middle of our observations. Then the variance weighted average of the positions of all detected features was calculated. The resulting average position of the masers in M33/19 and IC 133 are shown in Fig. 7 and Fig. 8 respectively. A fit of a rectilinear motion to these average positions yields motions of  $37 \pm 5 \mu\text{as yr}^{-1}$  in right ascension and  $-13 \pm 6 \mu\text{as yr}^{-1}$  in declination for M33/19. For IC 133 one gets a motion of  $3 \pm 3 \mu\text{as yr}^{-1}$  in right ascension and  $-13 \pm 10 \mu\text{as yr}^{-1}$  in declination. This is consistent with variance weighted average of all maser feature motions and suggests that the systematic internal motions within the two regions (e.g., outflow) are probably not a substantial source of bias with the current astrometric accuracy.

### 3 Geometric Distance of M33

The relative motions between M33/19 and IC 133 are independent of the proper motion of M33 and any contribution from the motion of the Sun. Since the rotation curve and inclination of the galaxy disk are known one can predict the expected relative angular motion of the two masing regions. The rotation of the HI gas in M33 has been measured by Corbelli & Schneider (1997), hereafter CS97. They fit a tilted-ring model to the measured velocities. According to their model of the rotation of M33, one can calculate the expected transverse velocities of M33/19 and IC 133. For M33/19, one expects a motion of  $42.4 \text{ km s}^{-1}$  in right ascension and  $-39.6 \text{ km s}^{-1}$  in declination. For IC 133 we expect  $-64.0 \text{ km s}^{-1}$  in right ascension and  $-74.6 \text{ km s}^{-1}$  in declination. This gives a relative motion of  $106.4 \text{ km s}^{-1}$  in right ascension and  $35 \text{ km s}^{-1}$  in declination between the two regions of maser activity.

The radial velocities of the  $\text{H}_2\text{O}$  masers in M33/19 and IC 133 and the proximate HI gas are in very good agreement ( $< 10 \text{ km s}^{-1}$ ). This strongly suggests that the maser sources are rotating with the HI gas in the galaxy. However, while the agreement between the rotation model presented by CS97 and the radial velocity of the HI gas at the position of IC 133 is also very good ( $< 5 \text{ km s}^{-1}$ ), there is a difference of  $\sim 15 \text{ km s}^{-1}$  at the position of M33/19. Hence, we conservatively assume a systematic error of  $20 \text{ km s}^{-1}$  in each velocity component for the relative velocity of the two maser components. Comparing the measured angular motion of  $30.8 \pm 4 \mu\text{as yr}^{-1}$  in right ascension with the expected linear motion of  $106 \pm 20 \text{ km s}^{-1}$ , one gets a geometric distance of

$$D = 730 \pm 100 \pm 135 \text{ kpc},$$

where the first error indicates the statistical error from the VLBI proper motion measurements while the second error is the systematic error from the rotation model.

After less than three years of observations, the uncertainty in the distance estimate is already dominated by the uncertainty of the rotation model of M33. However, this can be improved in the near future by better rotation models using higher resolution (e.g., Very Large Array or Westerbork Synthesis Radio Telescope) data of HI gas in the inner parts of the disk. Also, the precision of the proper motion measurements will increase with time as  $t^{3/2}$  for evenly spaced observations.

Within the current errors the geometric distance of  $730 \pm 100 \pm 135 \text{ kpc}$  is in good agreement with recent Cepheid and Tip of the Red Giant Branch (TRGB) distances of  $802 \pm 51 \text{ kpc}$  (Lee et al. 2002) and  $794 \pm 23 \text{ kpc}$  (McConnachie et al. 2004) respectively. It also agrees with a geometric distance estimate of  $800 \pm 180 \text{ kpc}$  obtained by Argon et al. (2004), who modeled the outflow within IC 133, as traced by  $\text{H}_2\text{O}$  maser proper motions estimated after a 14 year VLBI monitoring program. Other measurements using TRGB and Red Clump (RC) (Kim et al. 2002) favor a larger distance of  $916 \pm 55 \text{ kpc}$  and  $912 \pm 59 \text{ kpc}$  respectively.

## 4 Proper Motion of M33

The observed proper motion  $\vec{v}_{prop}$  of a maser (e.g., M33/19 or IC 133) in M33 can be decomposed into three components  $\vec{v}_{prop} = \vec{v}_{rot} + \vec{v}_{\odot} + \vec{v}_{prop}$ . Here  $\vec{v}_{rot}$  is the motion of the masers due to the internal galactic rotation in M33 and  $\vec{v}_{\odot}$  is the apparent motion of M33 caused by the rotation of the Sun around the Galactic Center. The last contribution  $\vec{v}_{prop}$  is the true proper motion of M33 relative to the Galaxy.

- The motion of the Sun can be decomposed into a circular motion of the Local Standard of Rest (LSR) and the peculiar motion of the Sun. Using a LSR velocity of  $236 \pm 15 \text{ km s}^{-1}$  (Reid & Brunthaler 2004) and the peculiar velocity of the Sun from Dehnen & Binney (1998), the motion of the Sun causes an apparent proper motion of  $\dot{\alpha}_{\odot} = 52.5 \pm 3.3 \mu\text{as yr}^{-1}$  in right ascension and  $\dot{\delta}_{\odot} = -37.7 \pm 2.4 \mu\text{as yr}^{-1}$  in declination, assuming a distance of 730 kpc and the Galactic coordinates of M33 ( $l = 133.6^\circ$ ,  $b = -31.3^\circ$ ).
- Using the rotation model of CS97, the contribution from the rotation of M33 (for IC 133) is  $\dot{\alpha}_{rot} = -18.5 \pm 6 \mu\text{as yr}^{-1}$  in right ascension and  $\dot{\delta}_{rot} = -21.6 \pm 6 \mu\text{as yr}^{-1}$  in declination. Here, we assumed again an uncertainty of  $20 \text{ km s}^{-1}$  for the rotation velocity and a distance of 730 kpc.
- Combining these velocity vectors, one gets the true proper motion of M33:

$$\begin{aligned} \dot{\alpha}_{prop} &= \dot{\alpha}_{prop} - \dot{\alpha}_{rot} - \dot{\alpha}_{\odot} \\ &= (4.7 \pm 3.2 + 18.5 \pm 6 - 52.5 \pm 3.3) \frac{\mu\text{as}}{\text{yr}} \\ &= -29.3 \pm 7.6 \frac{\mu\text{as}}{\text{yr}} = -101 \pm 35 \frac{\text{km}}{\text{s}} \\ \text{and} \\ \dot{\delta}_{prop} &= \dot{\delta}_{prop} - \dot{\delta}_{rot} - \dot{\delta}_{\odot} \\ &= (-14.1 \pm 6.4 + 21.6 \pm 6 + 37.7 \pm 1) \frac{\mu\text{as}}{\text{yr}} \\ &= 45.2 \pm 9.1 \frac{\mu\text{as}}{\text{yr}} = 156 \pm 47 \frac{\text{km}}{\text{s}}. \end{aligned}$$

The transverse velocity changes by less than  $5 \text{ km s}^{-1}$  if one uses the TRGB distance of  $794 \pm 23 \text{ kpc}$  (McConnachie et al. 2004) for this analysis. Finally, the systemic radial velocity of M33 is  $-179 \text{ km s}^{-1}$  (CS97). The radial component of the rotation of the Milky Way towards M33 is  $-140 \pm 9 \text{ km s}^{-1}$ . Hence, M33 is moving with  $-39 \pm 9 \text{ km s}^{-1}$  towards the Milky Way. This gives now the three dimensional velocity vector of M33 which is plotted in Fig. 9. The total velocity of M33 relative to the Milky Way is  $190 \pm 59 \text{ km s}^{-1}$ .

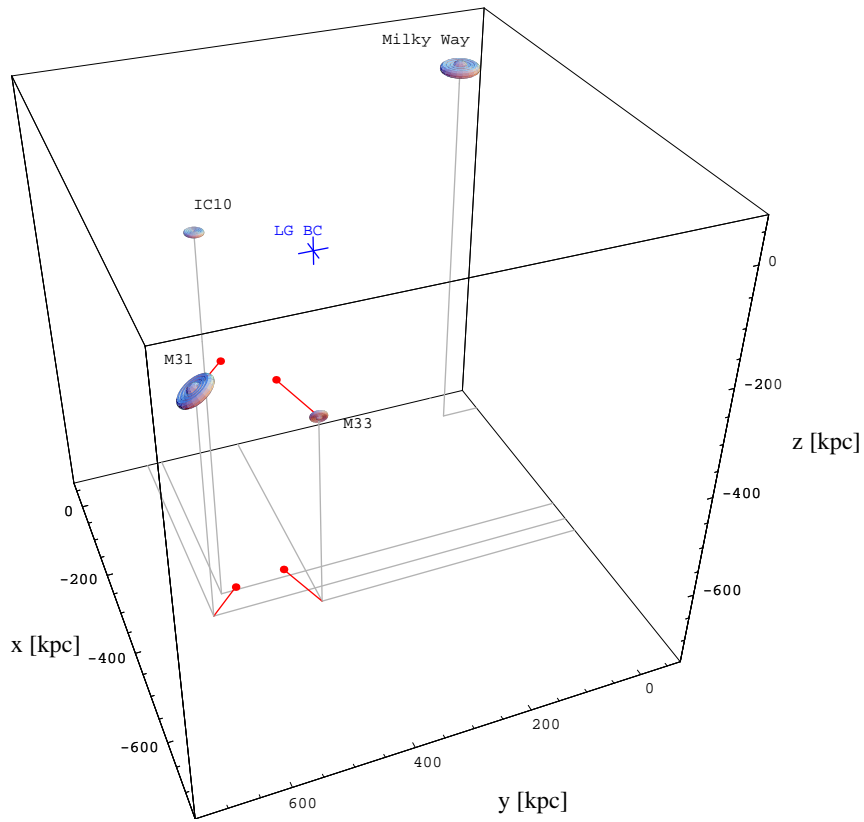


Figure 9: Schematic view of the Local Group with the space velocity of M33 and the radial velocity of Andromeda. The blue cross marks the position of the Local Group Barycenter (LG BC) according to van den Bergh (1999).

It is often argued (e.g. Kahn & Woltjer 1959) that the Milky Way is falling directly towards Andromeda (M31). This is based on the argument that there are no other large galaxies in the Local Group to generate angular momentum through tidal torques. Following this argument, we assume a zero proper motion of Andromeda. Then the angle between the velocity vector of M33 relative to Andromeda and the vector pointing from M33 towards M31 is  $30^\circ \pm 15^\circ$ . This angle strongly depends on the relative distance between Andromeda and M33. Thus, it is crucial to use distances for the two galaxies which have similar systematic errors. Thus, the TRGB distances to M33 and Andromeda from McConnachie et al. (2004) and McConnachie et al. (2005) respectively are used. For an angle of  $30^\circ$ , only elliptical orbits with eccentricities of  $e > 0.88$  are allowed. For the largest allowed angle of  $45^\circ$ , the eccentricities are restricted to  $e > 0.7$ . This eccentricity limit weakens if the proper motion of Andromeda is non-negligible and, for a motion of  $> 150$  km s $^{-1}$ , any eccentricity is allowed.

Gottesman, Hunter, & Boonyasait (2002) consider the effects of dynamical friction of Andromeda on M33. They conclude that Andromeda cannot have a very massive halo unless the orbit of M33 has a low eccentricity. Otherwise, the dynamical friction would have lead to a decay of the orbit of M33. If this is correct, then the high eccentricity of the orbit of M33 would lead to the conclusion that the total mass of Andromeda must be less than  $10^{12} M_\odot$ . This is in good agreement with recent estimates by Evans & Wilkinson (2000) and Evans et al. (2003) ( $\sim 1.2 \times 10^{11} M_\odot$ ) derived from the three-dimensional positions and radial velocities of its satellite galaxies.

The next step towards a kinematic model of the Local Group is a model of the Andromeda subgroup. If one assumes that M33 is bound to Andromeda, a lower limit on the mass of Andromeda can be estimated by comparing the relative speed with the escape velocity. This mass limit still depends on the unknown proper motion vector of Andromeda. However, some proper motion vectors can be excluded for Andromeda, since it would lead to scenarios in which M33 would have been destroyed by the close interaction with Andromeda. Similar same arguments can be made for IC 10.

## 5 Discussion & Outlook

More than 80 years after van Maanen's observation, we have succeeded with measuring the rotation and proper motion of M33. These measurements provide a new handle on dynamical models for the Local Group and the mass and dark matter halo of Andromeda and the Milky Way.

Further VLBI observations within the next few years and an improved rotation model have the potential to improve the accuracy of the distance estimate to less than 10%. At least one additional maser source exists in M33 (M33/50, see Huchtmeier, Eckart, & Zensus 1988) that will be used in the future to increase the accuracy of the measurements. A third region of maser activity will also help to check for non-circular velocities of the masers.

Unfortunately, no maser emission could be found in Andromeda despite intensive searches (e.g., Imai et al. 2001). Hence, the proper motion vector of Andromeda is still unknown. In the near future, new technical developments using higher bandwidths will increase the sensitivity of VLBI. This will allow the detection of radio emission from the central black hole of Andromeda, M31\*, with flux densities of  $\sim 30 \mu\text{Jy}$  (Crane, Dickel, & Cowan 1992), to measure the proper motion of Andromeda. Today we are only able to study the extreme (bright) tip of the maser luminosity distribution for interstellar masers. The Square Kilometer Array (SKA), with substantial collecting area on intercontinental baselines and a frequency coverage up to 22 GHz (Fomalont & Reid 2004), will provide the necessary sensitivity to detect and measure the proper motions of a much greater number of masers in active star forming regions in the Local Group.

## Acknowledgements

The VLBA is operated by the National Radio Astronomy Observatory (NRAO). The National Radio Astronomy Observatory is a facility of the National Science Foundation operated under cooperative agreement by Associated Universities, Inc.

## References

- Argon A. L., Greenhill L. J., Moran J. M., et al., 1994, *ApJ*, 422, 586
- Argon A. L., Greenhill L. J., Moran J. M., et al., 2004, *ApJ*, 615, 702
- Becker R., Henkel C., Wilson T. L., Wouterloot J. G. A., 1993, *A&A*, 268, 483
- Brunthaler A., Reid M., Falcke H., Greenhill L. J., Henkel C., 2002, Towards Proper Motions in the Local Group, in *Proceedings of the 6th EVN Symposium*, p. 189
- Brunthaler A., Reid M. J., Falcke H., 2005, Atmosphere-Corrected Phase-Referencing, in *ASP Conf. Ser. 340: Future Directions in High Resolution Astronomy*, p. 455
- Brunthaler A., Reid M. J., Falcke H., Greenhill L. J., Henkel C., 2005, *Science*, 307, 1440
- Corbelli E., Schneider S. E., 1997, *ApJ*, 479, 244
- Courteau S., van den Bergh S., 1999, *AJ*, 118, 337
- Crane P. C., Dickel J. R., Cowan J. J., 1992, *ApJ*, 390, L9
- Dehnen W., Binney J. J., 1998, *MNRAS*, 298, 387

Eckart A., Genzel R., 1996, *Nat.*, 383, 415

Eisenhauer F., Schödel R., Genzel R., et al., 2003, *ApJ*, 597, L121

Evans N. W., Wilkinson M. I., 2000, *MNRAS*, 316, 929

Evans N. W., Wilkinson M. I., Perrett K. M., Bridges T. J., 2003, *ApJ*, 583, 752

Fich M., Tremaine S., 1991, *ARA&A*, 29, 409

Fomalont E., Reid M., 2004, *New Astronomy Review*, 48, 1473

Freedman W. L., 2000, *Phys. Rep.*, 333, 13

Ghez A. M., Duchêne G., Matthews K., et al., 2003, *ApJ*, 586, L127

Gottesman S. T., Hunter J. H., Boonyasait V., 2002, *MNRAS*, 337, 34

Greenhill L. J., Moran J. M., Reid M. J., et al., 1990, *ApJ*, 364, 513

Greenhill L. J., Moran J. M., Reid M. J., Menten K. M., Hirabayashi H., 1993, *ApJ*, 406, 482

Herrnstein J. R., Moran J. M., Greenhill L. J., et al., 1999, *Nat.*, 400, 539

Hubble E. P., 1926, *ApJ*, 63, 236

Huchtmeier W. K., Eckart A., Zensus A. J., 1988, *A&A*, 200, 26

Imai H., Ishihara Y., Kameya O., Nakai N., 2001, *PASJ*, 53, 489

Israel F. P., van der Kruit P. C., 1974, *A&A*, 32, 363

Jones B. F., Klemola A. R., Lin D. N. C., 1994, *AJ*, 107, 1333

Kahn F. D., Woltjer L., 1959, *ApJ*, 130, 705

Kim M., Kim E., Lee M. G., Sarajedini A., Geisler D., 2002, *AJ*, 123, 244

Kobayashi H., Ishiguro M., Chikada Y., et al., 1989, *PASJ*, 41, 141

Kochanek C. S., 1996, *ApJ*, 457, 228

Kulesa A. S., Lynden-Bell D., 1992, *MNRAS*, 255, 105

Lee M. G., Kim M., Sarajedini A., Geisler D., Gieren W., 2002, *ApJ*, 565, 959

McConnachie A. W., Irwin M. J., Ferguson A. M. N., et al., 2004, *MNRAS*, 350, 243

McConnachie A. W., Irwin M. J., Ferguson A. M. N., et al., 2005, *MNRAS*, 356, 979



Mould J. R., Huchra J. P., Freedman W. L., et al., 2000, *ApJ*, 529, 786

Newman J. A., Ferrarese L., Stetson P. B., et al., 2001, *ApJ*, 553, 562

Ngeow C., Kanbur S. M., 2004, *MNRAS*, 349, 1130

Reid M. J., 1993, *ARA&A*, 31, 345

Reid M. J., Argon A. L., Masson C. R., Menten K. M., Moran J. M., 1995, *ApJ*, 443, 238

Reid M. J., Brunthaler A., 2004, *ApJ*, 616, 872

Reid M. J., Readhead A. C. S., Vermeulen R. C., Treuhaft R. N., 1999, *ApJ*, 524, 816

Sandage A., Tammann G. A., Reindl B., 2004, *A&A*, 424, 43

Schödel R., Ott T., Genzel R., et al., 2002, *Nat.*, 419, 694

Schweitzer A. E., Cudworth K. M., Majewski S. R., Suntzeff N. B., 1995, *AJ*, 110, 2747

Shaya E. J., Tully R. B., Peebles P. J. E., et al., 2003, Space interferometry mission dynamical observations of galaxies (SIMDOG) key project, in *Interferometry in Space*. Edited by Shao, Michael. Proceedings of the SPIE, Volume 4852, pp. 120-130 (2003)., p. 120

Steigman G., Tkachev I., 1999, *ApJ*, 522, 793

Tammann G. A., Sandage A., Reindl B., 2003, *A&A*, 404, 423

van den Bergh S., 1999, *A&A Rev.*, 9, 273

van Maanen A., 1923, *ApJ*, 57, 264

Walker R. C., Burke B. F., Johnston K. J., Spencer J. H., 1977, *ApJ*, 211, L135